Model of the Height Variation of the Turbulence Kinetic Energy Budget in the Unstable Planetary Boundary Layer

D. H. LENSCHOW

National Center for Atmospheric Research,[1] *Boulder, Colo. 80302*

(Manuscript received 2 July 1973, in revised form 9 October 1973)

ABSTRACT

A model is proposed for the variation with height of the terms in the turbulence kinetic energy budget throughout an unstably stratified barotropic planetary boundary layer. The model is based upon aircraft measurements throughout the boundary layer that are presented here and previous results from surface layer measurements. The model assumes that at the limit of neutral stability, the transport term in the budget equation is at a minimum. When the height above the ground is greater than about ten times the absolute value of the Obukhov length, the shear-generation term is negligible, while the rate of dissipation of turbulence energy becomes almost constant, and the transport term increases almost linearly with height to balance the almost linear decrease of the buoyancy-generation term. Measurements of the ratio of the vertical flux of the horizontal part of the turbulence kinetic energy to the vertical part show good agreement with a model based upon surface layer observations and a laboratory tank experiment.

One set of observations was taken over a lake from just downwind of the shore to about 30 km offshore and the assumption of horizontal homogeneity was found to be unjustified.

1. Introduction

Few measurements have been reported of the important terms in the turbulence kinetic energy budget in a convective boundary layer above the surface layer. Instrumented aircraft have been used for direct measurements of some of the terms by, for example, Myrup (1969), Zubkovskiy and Koprov (1970) and Lenschow (1970). In the last two studies the generation of turbulence by buoyancy was measured directly. The rate of dissipation of turbulence energy was estimated in all three studies from the magnitude of the spectral densities in the inertial subrange using empirically derived values for the Kolmogoroff constant. In the first two studies the vertical transport of turbulence kinetic energy and pressure fluctuations was estimated as the residual term balancing the buoyancy-generation and dissipation terms, while Lenschow (1970) measured the vertical transport of turbulence energy directly. Sheih *et al.* (1971) measured viscous dissipation directly from an aircraft, but did not report measurements through the entire boundary layer. Estimates of the rate of dissipation using Kolmogoroff's hypothesis were obtained from a tethered balloon by Rayment (1973). Measurements were obtained throughout the boundary layer although the depth of the boundary layer was not reported.

[1] The National Center for Atmospheric Research is sponsored by the National Science Foundation.

In the surface layer, Wyngaard and Coté (1971) have made a detailed study of the turbulence kinetic energy budget. They used direct measurements of turbulence energy production by both shear and buoyancy, the vertical transport of turbulence, and the rate of viscous dissipation. Thus, their residual term, or imbalance, can be ascribed either to the vertical transport of pressure fluctuations, which was not measured, or to experimental difficulties such as horizontal inhomogeneity.

In this paper, a model of the variation with height of the terms in the turbulence kinetic energy equation in a convectively unstable barotropic boundary layer is presented, based on an extrapolation of the surface layer formulations developed by Wyngaard and Coté (1971), as well as on aircraft observations throughout the boundary layer above the surface layer.

2. Model of turbulence kinetic energy budget

The turbulence kinetic energy budget in the boundary layer is given by

$$\frac{\partial \bar{e}'}{\partial t} = \frac{g}{T}\overline{w'T_v'} - \frac{\partial}{\partial z}\overline{w'(e'+p'/\rho)} + \frac{1}{\rho}\overline{\boldsymbol{\tau}\cdot\frac{\partial \mathbf{V}}{\partial z}} - \bar{u}\frac{\partial \bar{e}'}{\partial x} - \epsilon, \quad (1)$$

where $\bar{e}'$ is the kinetic energy, $\frac{1}{2}(\overline{u'^2}+\overline{v'^2}+\overline{w'^2})$, $\boldsymbol{\tau}$ the stress, $\partial\bar{\mathbf{V}}/\partial z$ the vertical shear, ϵ the viscous energy dissipation, g the gravitational acceleration, T_v the virtual temperature, and ρ the density. The prime

indicates a departure from the mean value and the overbar indicates a mean value over the length of the measurement run. The direction of the x axis is defined to be in the direction of the mean wind. For the measurements discussed here, this direction is the average direction over all the flight levels. The time rate of change of kinetic energy is almost two orders of magnitude smaller than the other terms. The horizontal advection term, $-\bar{u}\partial\overline{e'}/\partial x$, cannot be measured from a fixed point and is usually assumed to be negligible for surface layer measurements. The aircraft measurements generally support this assumption, although one case was purposely selected (and discussed later) which was not horizontally homogeneous to investigate this assumption. Rewriting (1), incorporating these assumptions, and dropping the subscript on virtual temperature, we have

$$\frac{g}{T}\overline{w'T'}-\frac{\partial}{\partial z}\overline{w'(e'+p'/\rho)}+\frac{1}{\rho}\overline{\tau\cdot\frac{\partial\bar{V}}{\partial z}}-\epsilon=0. \tag{2}$$

In order to effectively model the turbulence energy budget throughout the boundary layer, we use as a starting point our present knowledge of the surface layer, or constant flux layer, which is the source of the vertical turbulent fluxes of heat and kinetic energy and the sink of momentum flux for the part of the boundary layer above the surface layer.

Wyngaard and Coté (1971) have parameterized the terms in the turbulence energy equation in terms of surface layer similarity theory, which predicts that the terms should be universal functions of z/L, where z is the height above the surface and L the Obukhov length, defined in terms of surface layer variables (denoted by the subscript 0) as

$$L=\frac{-u_*^3T}{kg(\overline{w'T'})_0}.$$

The friction velocity is $u_*=\sqrt{(-\overline{u'w'})_0}$ and k the von Kármán constant. Businger *et al.* (1971) suggest the value $k=0.35$ which was used here. For unstable conditions, Wyngaard and Coté (1971) indicate that their analysis seems to apply when $-z/L<1.0$. The aircraft measurements at the lowest level on two of the days presented here were within this range. Therefore, their results can be used for comparison and for interpolation of the terms in the equation measured at the lowest aircraft flight level down to the surface. The values they obtained for these terms are as follows:

$$\overline{u'w'}\frac{\partial\bar{u}}{\partial z}=\frac{u_*}{kz}\overline{u'w'}\left(1-\frac{15z}{L}\right)^{-\frac{1}{4}} \tag{3a}$$

$$\frac{\partial\overline{w'e'}}{\partial z}\approx\frac{u_*^3}{kz}\frac{z}{L}=-\frac{g}{T}\overline{w'T'} \tag{3b}$$

$$\epsilon=\frac{u_*^3}{kz}\left(1+0.5\left|\frac{z}{L}\right|^{\frac{2}{3}}\right)^{\frac{3}{2}}. \tag{3c}$$

We will now develop expressions for these terms in an unstable barotropic boundary layer above the surface layer, where the fluxes of momentum, kinetic energy and buoyancy, as well as the kinetic energy itself, vary with height and approach zero at the top of the boundary layer. Above the surface layer, $\partial\bar{V}/\partial z$ becomes small and thus $(1/\rho)\overline{\tau\cdot(\partial\bar{V}/\partial z)}$ is not a significant term, compared to the buoyancy term. Therefore, all the terms in the kinetic energy equation are normalized by the buoyancy flux near the surface, $(g/T)(\overline{w'T'})_0$.

The normalized terms in the kinetic energy equation, obtained by dividing (2) by the surface buoyancy flux, are defined as

$$H+T_r+S-D=0, \tag{4}$$

where H and S are the buoyancy- and shear-generation terms, T_r the divergence of the vertical transport of turbulence energy and pressure fluctuations, and D the dissipation.

Assuming horizontal homogeneity and negligible radiative cooling,

$$\frac{\partial\bar{T}}{\partial t}=-\rho c_p\frac{\partial\overline{w'T'}}{\partial z}. \tag{5}$$

Since the vertical temperature structure is observed to remain constant above the surface layer and below the base of the inversion at the top of the boundary layer through the unstable part of the day,

$$\frac{\partial}{\partial z}\left(\frac{\partial\bar{T}}{\partial t}\right)=-\rho c_p\frac{\partial^2\overline{w'T'}}{\partial z^2}=0, \tag{6}$$

or

$$H\equiv\frac{\overline{w'T'}(z_*)}{(\overline{w'T'})_0}=az_*+b, \tag{7}$$

where a and b are constants and $z_*=z/z_i$. The height z_i is the top of the boundary layer, which is defined as the point at which the buoyancy flux is a minimum. Since $\partial\overline{w'T'}/\partial z=0$ at this level, $\partial\bar{T}/\partial t=0$ at $z=z_i$. This seems to also coincide with the point of maximum rate of decrease of kinetic energy and viscous dissipation with height.

Eq. (7) may not apply within the surface layer, since $\partial\bar{T}/\partial z+g/c_p$ is a function of $-z/L$, and therefore changes with changing surface heat flux and mean wind.

The top of the boundary layer measured instantaneously at a point by an ascending aircraft is often distinguishable to within a few meters by the abrupt decrease in turbulence and increase in temperature.

However, over a horizontal traverse, the aircraft may be alternatively above and below the corrugated surface of the inversion base, and increasing or decreasing the height of the flight path may only change the percent of time that the aircraft is above or below the local inversion. The result of this horizontal averaging is a smearing of the average height of the inversion, and of the region of significant transfer of turbulence fluxes.

Entrainment of warmer air above the inversion into the mixed air of the boundary layer results in a slightly negative buoyancy flux near the top of the boundary layer. Measurements by Lenschow (1970, 1973) indicate that this negative flux is less than 10% of the surface value. Laboratory studies of convection by Deardorff *et al.* (1968) indicated a value of $<6\%$, while recent numerical results of Deardorff (unpublished) indicate a value of about 12%. Both results also indicate that the flux is zero somewhere between $z_*=0.85$ and 0.90, and is approximately linear with height up to this level.

Combining these observations, we have for the region of positive flux

$$H=1-1.15z_*, \quad 0<z_*\leqslant 0.87.$$

At $z_*=0.87$, $H=0$ and $\partial H/\partial z_*=-1.15$; at $z_*=1.0$, $H=-0.1$ and $\partial H/\partial z_*=0$. This is sufficient to evaluate the first four terms of a power series expansion for H:

$$H=-13.81+49.96z_*-58.78z_*^2+22.53z_*^3,$$
$$=h(z_*), \quad 0.87\leqslant z_*\leqslant 1.$$

Therefore,

$$H=\begin{cases}1-1.15z_*, & 0\leqslant z_*\leqslant 0.87\\ h(z_*), & 0.87\leqslant z_*\leqslant 1\end{cases} \tag{8}$$

The average value of H through the entire boundary layer, obtained by integrating (8) from $z_*=0$ to $z_*=1$, is $\langle H\rangle=0.43$.

The normalized shear-generation term in the surface layer is

$$S=\frac{(\overline{u'w'})_0}{u_*^2}\frac{L}{z}\left(1-\frac{15z}{L}\right)^{-\frac{1}{4}}=\frac{(\overline{u'w'})_0}{u_*^2}\frac{L}{z_i}\frac{\left(1-15\frac{z_i}{L}z_*\right)^{-\frac{1}{4}}}{z_*}. \tag{9}$$

Above the surface layer, the normalized shear generation is given by the negative of the inverse of the flux Richardson number,

$$S=-\mathrm{Rf}^{-1}=\frac{-T\overline{u'w'}\dfrac{\partial\bar{u}}{\partial z}}{g\overline{w'T'}}. \tag{10}$$

The variation of $-\overline{u'w'}$ with height above the surface layer is not, in general, known. In fact, its variation with height is probably greatly dependent upon the variation of the wind with height in the vicinity of the top of the mixed layer and upon the time rate of change of the height of the mixed layer. In comparison with the wind shear in the surface layer, however, the wind shear throughout the rest of the mixed layer, except perhaps near the top, is very small. Therefore, regardless of what we assume for a height variation of $-\overline{u'w'}$, the shear generation is not greatly affected. Similarly, since $\partial\bar{v}/\partial z$ is small compared to $\partial\bar{u}/\partial z$ in the surface layer, $\overline{v'w'}\partial\bar{v}/\partial z$ contributes very little to the kinetic energy budget in comparison with the buoyancy term. According to Deardorff's (1972) numerical results, this is true as long as $-z_i/L>3$. Near the top of the mixed layer, however, the shear may again increase. Since this depends upon the difference in wind above and below the top of the mixed layer and the rate of entrainment of air from above the top of the mixed layer, this will not be considered further here.

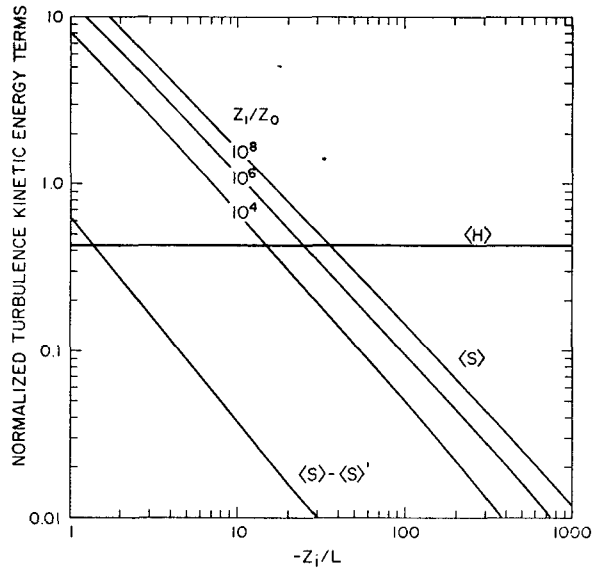

FIG. 1. The normalized shear-generation term ($\langle S\rangle$) integrated over the entire boundary layer for values of z_i/z_0 from 10^4 to 10^8, assuming the stress is constant throughout the boundary layer. The difference between this and the integrated shear-generation term, assuming a linear decrease in stress with height to zero at the top of the boundary layer, is also plotted ($\langle S\rangle-\langle S\rangle'$). The buoyancy-generation term ($\langle H\rangle$) is shown for reference.

As an example, we assume below in case (a) that $-\overline{u'w'}$ is constant with height throughout the mixed layer ($-\overline{u'w'}=u_*^2$) and in case (b) that it decreases linearly with height to zero at the top of the mixed layer [$-\overline{u'w'}=u_*^2(1-z_*)$], in both cases using the surface layer formulation for wind shear and assuming that the stress and shear vectors are aligned. Integrating (9) through the entire boundary layer under these assumptions and averaging, we have

$$\text{(a)} \qquad \langle S\rangle=-\frac{L}{z_i}\left[\ln\frac{z_i}{z_0}-\psi_1(x)\right], \tag{11a}$$

$$\text{(b)} \qquad \langle S\rangle'=\langle S\rangle-\frac{4}{45}\left(\frac{-L}{z_i}\right)^2(x^3-1), \tag{11b}$$

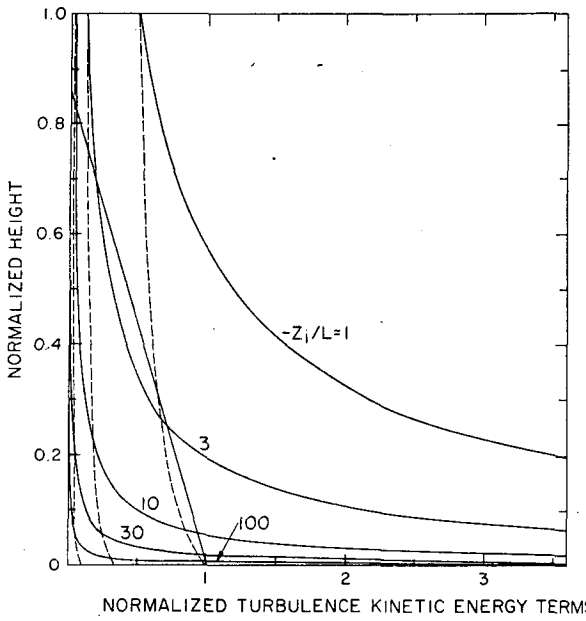

FIG. 2. The normalized shear-generation term as a function of height for values of $-z_i/L=1$, 3, 10, 30 and 100. The dashed lines which intersect the shear-generation term at $z_*=1.0$ are the difference between the shear-generation term assuming a constant stress and the shear-generation term assuming a linearly decreasing stress with height. The normalized buoyancy term (the straight line that intersects 0 and 1 at $z_*=0.83$ and 0, respectively) is also plotted.

where

$$x=(1-15z_i/L)^{\frac{1}{4}},$$

$$\psi_1(x)=2\ln\frac{1+x}{2}+\ln\frac{1+x^2}{2}-2\tan^{-1}x+\frac{\pi}{2},$$

and z_0 is the surface roughness length. The expression for ψ_1 was obtained by Paulson (1970) in deriving an expression for the wind profile in the surface layer.

These terms are plotted in Fig. 1 as a function of $-z_i/L$ for several values of z_i/z_0. In this figure, $\langle S\rangle-\langle S\rangle'$ is everywhere less than 8% of $\langle S\rangle$. In Fig. 2, S is plotted as a function of height for several values of $-z_i/L$. We see, for example, that at $z_*=0.1$ and $-z_i/L=30$, the shear-generation term contributes less than 15% of the buoyancy term to the generation of turbulence energy. Therefore, the shear-generation term is only slightly affected by the assumed variation of $-\overline{u'w'}$ with height. We assume here that it is constant with height through the entire boundary layer, i.e.,

$$S=-L/z_i\frac{[1-15(z_i/L)z_*]^{-\frac{1}{4}}}{z_*}. \tag{12}$$

The normalized viscous dissipation in the surface layer, obtained from direct measurements and reported by Wyngaard and Coté (1971), is given by

$$D=-L/z[1+0.5(z/-L)^{\frac{2}{3}}]^{\frac{3}{2}}$$

$$=-L/z_i\frac{[1+0.5(z_i/-L)^{\frac{2}{3}}z_*^{\frac{2}{3}}]^{\frac{3}{2}}}{z_*}. \tag{13}$$

The aircraft observations presented later indicate that D decreases slowly with height and approaches a constant in the unstable boundary layer above the surface layer. This is not inconsistent with Myrup's (1969) measurements. Zubkovskiy and Koprov (1970) and Rayment (1973) show a decrease of D with height, but, since they did not normalize the height by z_i this may be due to the averaging together of cases of different boundary layer heights. We note that (13) does approach a constant, namely, $(0.5)^{\frac{3}{2}}=0.35$ as $-z/L\to\infty$. However, the dissipation exceeds the total production $(S+H)$ for values of $-z/L<1.95$. This is puzzling in view of the observations by Wyngaard and Coté (1971) that the divergence of the vertical transport of kinetic energy in the surface layer is approximately equal to the negative of the buoyancy flux. Integrating their expression for D through the entire boundary layer, we find that $\langle D\rangle>\langle(S+H)\rangle$ for all values of $-z_i/L<336$.

Wyngaard and Coté (1971) assumed that as $-z/L\to 0$, the dissipation is equal to the production. Measurements by Laufer (1950) indicate that this is not true in a wind tunnel. Therefore, it is likely that even for neutral stability, some of the shear-generated turbulence energy is transported upward and dissipated at the higher levels in the boundary layer. Airplane observations indicate that the transport term is negative in the lower part of the boundary layer and positive in the upper part. Integrated over the entire boundary layer, this term is zero, since it is a transport term and does not generate or dissipate kinetic energy.

There are no direct observations of the pressure term through the surface layer or the rest of the boundary layer. Numerical results for very unstable conditions indicate, however, that above the surface layer this term is relatively small. Deardorff (1972) found that the pressure term was 0.2–0.4 times the negative of the transport term. (Later unpublished results by Deardorff indicate that for the time-dependent boundary layer the contribution of the pressure term is even less than this.) Within the surface layer, the results are not clear, so that a part of the discrepancy in Wyngaard and Coté's data may be due to the pressure term. Since this term appears to be small above the surface layer and is zero when integrated over the entire boundary layer, it appears that their observed imbalance cannot be entirely due to this unmeasured term.

In summary, we have the following conditions that a model of D must fulfill in an unstable boundary layer:

(1) D is nearly constant with height and S is negligible in the upper or convective part of the boundary layer ($z \gg |L|$).
(2) $D=H+S+T_r$.
(3) $\langle D\rangle=\langle H\rangle+\langle S\rangle$.
(4) as $-z_i/L\to\infty$, $\langle D\rangle=\langle H\rangle=0.43$.
(5) as $-z/L\to 0$, $Dz/-L<1$.
(6) $\partial D/\partial z\leqslant 0$.

These conditions are fulfilled by the following assumption for dissipation:

$$D=H+S+a(\langle S\rangle-S)+b(\langle H\rangle-H).$$

By condition (1), $b\approx 1$, so that

$$D=0.43+a(\langle S\rangle-S)+S, \tag{14a}$$

and from (4) it follows that

$$T_r=0.43+a(\langle S\rangle-S)-H. \tag{14b}$$

In the absence of more specific knowledge of what fraction of the shear-generated turbulence is dissipated locally and what fraction is transported to another level, we assume that a is a constant and $0<a<1$. The limiting case of $a=0$, which is plotted in Fig. 3 after multiplying D by $z/-L$ and T_r by z/L to make it compatible with surface layer scaling, is equivalent to assuming that as $-z/L\to 0$, $Dz/-L=1$. For the limiting case of $a=1$, D is constant throughout the entire boundary layer.

Wyngaard and Coté's (1971) results indicate that for stable stratification, their transport term (which does not include pressure fluctuations) is small, with no clearly defined functional dependence upon z/L. Therefore, we would expect that as $-z/L\to 0$, the slope of the transport term is small. We would not expect the slope of the transport term to be <0 for $-z/L>0$, since this would mean that at any given height the transport of turbulence energy is greater at neutral stability than at slightly unstable stability. This is unlikely, in view of the increased effectiveness of vertical transport in an unstable boundary layer.

The dissipation term ($Dz/-L$), on the other hand, depends upon the local intensity of small-scale turbulence. It seems reasonable that the dissipation is somewhat greater at neutral stability than for slightly unstable conditions since more of the turbulence that is generated locally may be dissipated locally at neutral stability.

Furthermore, Wyngaard and Coté (1971) observed that the normalized dissipation term increases rapidly for $-z/L<0$. There is no reason to believe that the minimum value of dissipation occurs at $z/L=0$, and therefore no basis for specifying the slope at this point. The total production of energy in the surface layer (normalized by u_*^3/kz) reaches a minimum of 0.78 at $-z/L=0.31$ and has a slope of -3.3 at $-z/L=0$.

On this basis, we select $a=0.57/(\langle S\rangle+3.75)$, which is the value required to set $\partial(T_r z/L)/\partial(-z/L)=0$ at

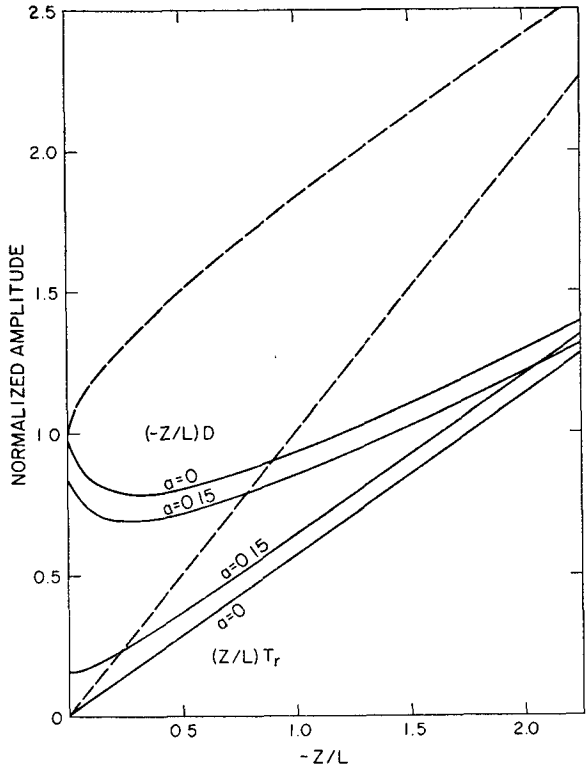

FIG. 3. Normalized dissipation $[(-z/L)D]$ and transport $[(z/L)T_r]$ terms in the turbulence energy equation plotted as functions of $-z/L$ for $a=0$ and 0.15 and $\langle S\rangle=z/z_i=0$. The dashed lines are Wyngaard and Coté's (1971) formulations.

$-z/L=0$. Substituting this value of a into (14), we have

$$\left.\begin{aligned} D&=0.43+\frac{0.57}{\langle S\rangle+3.75}(\langle S\rangle-S)+S\\ T_r&=0.43+\frac{0.57}{\langle S\rangle+3.75}(\langle S\rangle-S)-H\end{aligned}\right\}. \tag{15}$$

We note that for $\langle S\rangle\leqslant 0.3$, D can be approximated to an accuracy of better than 9% and T_r to about 8% of its value at the surface by

$$\left.\begin{aligned} D&=0.43+0.15\langle S\rangle+0.85S\\ T_r&=0.43+0.15(\langle S\rangle-S)-H\end{aligned}\right\}. \tag{16}$$

Since the formulations for D and T_r depend explicitly upon S, the equations can still be used with different formulations for S. For example, in a baroclinic atmosphere the shear may be quite different from and larger in magnitude than that predicted by the surface layer theory.

Thus, Eqs. (8), (12) and (15) provide a formulation for all the significant terms in a horizontally homogeneous unstable boundary layer, from the surface up to the top of the mixed layer. In Fig. 3 the formulations

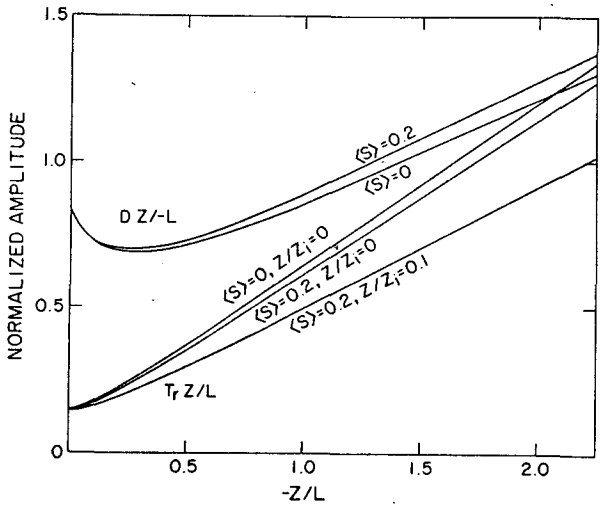

FIG. 4. Normalized dissipation $[(-z/L)D]$ and transport $[(z/L)T_r]$ terms for $a=0.15$, $\langle S\rangle=0$ and 0.2, and $z/z_i=0$ and 0.1.

for dissipation and transport for $a=0$ and 0.15 and $\langle S\rangle=z/z_i=0$ are compared with the surface-layer formulations of Wyngaard and Coté (1971) as functions of $-z/L$. Fig. 4 has plots of dissipation and transport for $a=0.15$, $\langle S\rangle=0$ and 0.2, and $z/z_i=0$ and 0.1. We see that, with the exception of the region close to neutral, the formulations proposed here for both terms are about half as large as the formulations they proposed. The smaller values of T_r and D are necessary to balance the energy equation. We note, however, that T_r here represents both pressure fluctuations and turbulence energy transport, whereas Wyngaard and Coté's transport term includes only turbulence energy.

3. Measurement sites and techniques

Three sets of aircraft measurements of terms in the turbulence kinetic energy budget are presented here: 1) a flight over the Great Plains of eastern Colorado on 25 April 1968 described in detail (including a plot of the turbulence energy budget) by Lenschow (1970), 2) a flight over the upwind end of Lake Michigan on 5 November 1970, and 3) a flight over the middle of Lake Huron on 13 November 1970. The meteorological conditions that existed during the two Great Lakes flights are discussed by Lenschow (1973). These are both examples of relatively cold air passing over the warmer water of the lakes. Compared to a land surface the lake is a relatively homogeneous surface although as pointed out by Lenschow (1973), surface temperature variations of up to 3C that existed on 5 November caused horizontal variations in the turbulence energy and heat and water vapor fluxes. In addition, the measurements on this day were taken over the upwind end of the lake. As a result, the horizontal advection of turbulence was not a negligible term in the turbulence energy budget.

On the other hand, the horizontal advection of turbulence was found to be negligible on 13 November, since the measurements were taken over the middle of the lake more than 50 km from the upwind shore and the surface temperature was quite uniform across the lake.

The flight pattern consisted of an alongwind and crosswind leg at each of several levels within the boundary layer. The flight path at each successive level was along the opposite direction of the preceding level, so that after completing two levels, the airplane was back to its initial position. The duration of each leg was about 5 min, which amounts to about 22 km in length. On 25 April, the entire pattern was immediately repeated at the same levels and the results shown are the average of the two sets of runs.

The air velocity components were obtained from the sum of (i) measurements of the velocity of the air with respect to the airplane and (ii) measurements of the velocity and angular orientation of the airplane with respect to the earth. Incidence angle vanes were used to measure the lateral and vertical components and a pitot-static tube for the longitudinal component of (i). An inertial navigation system was used over the Great Lakes to measure (ii), while a Doppler radar and a gyroscopically stabilized platform containing a vertically oriented accelerometer were used over eastern Colorado. Air temperature was obtained from the resistance of a 0.0025-cm tungsten wire exposed to the airstream. Details of the equipment and the methods of obtaining velocities and temperature from the aircraft measurements are described by Lenschow (1970, 1971, 1972). Measurements of humidity fluctuations were obtained from a microwave cavity refractometer, after correcting for the temperature and pressure dependencies of the measured refractivity.

The sample rate used for the calculations was 8 samples $\sec^{-1}$, which is equivalent to a wavelength of between 9 and 10 m. Before calculating any of the fluxes or spectra, a linear trend was removed from each of the variables by a least-squares fit.

Measurements of the production of energy by buoyancy were obtained from

$$\frac{g}{T}\overline{w'T_v'}=\frac{g}{T}\overline{w'T'}+0.61g\overline{w'q'}, \tag{17}$$

where T_v is the virtual temperature and q the specific humidity. At the lowest flight levels over the Great Lakes the contribution of the water vapor flux to the buoyancy term is about 10% of the sensible heat flux term. The relative contribution of the water vapor flux increases with height, however, since the sensible heat flux crosses zero and has a small negative value near the top of the boundary layer whereas the water vapor flux remains positive throughout the boundary layer. This is because the specific humidity above the boundary layer is less than that within the boundary

layer while the potential and the equivalent potential temperature is greater above the boundary layer. (In the regions where the top of the boundary layer is cloud-covered, the equivalent potential temperature is conserved during entrainment; in clear air, potential temperature is conserved.) Therefore, entrainment of air into the boundary layer from above results in a negative sensible heat flux and a positive water vapor flux near the top of the boundary layer. On the 25 April flight over eastern Colorado, water vapor flux was not measured. Its contribution to the buoyancy term, however, was estimated to be considerably smaller than it was over the Great Lakes.

The shear-production term was estimated by calculating the difference in wind between two adjacent flight levels separated by a height increment Δz and multiplying each component of shear by the respective component of stress, i.e.,

$$\frac{1}{\rho}\boldsymbol{\tau}\cdot\frac{\partial \mathbf{V}}{\partial z}\approx \overline{u'w'}\frac{\Delta\bar{u}}{\Delta z}+\overline{v'w'}\frac{\Delta\bar{v}}{\Delta z}. \tag{18}$$

The stress was obtained from the average of the stress measured at both levels and in both the alongwind and crosswind directions. Since the difference in wind velocity between two adjacent flight levels is typically 1 m sec^{-1}, or less, and the scatter in measurements of $\overline{u'w'}$ and $\overline{v'w'}$ is greater than for a quantity such as $\overline{w'T'}$, the estimates of shear production show more scatter than buoyancy production.

Estimates of u_* were obtained from measured values of $[(\overline{u'w'})^2+(\overline{v'w'})^2]^{\frac{1}{4}}$ averaged over the lowest two flight levels, in order to include in the average for u_* measurements along all four flight directions. This is because systematic errors that may occur in the measurement of the longitudinal velocity component (with respect to the aircraft) will also appear in the vertical and lateral velocity components, since these two components are calculated approximately from the product of true air speed (from which the longitudinal velocity component is calculated) and the angle of the air flow. Therefore, $\overline{u'w'}$ and $\overline{v'w'}$ may contain a systematic bias related to the direction of flight, which would be removed by averaging along all four directions.

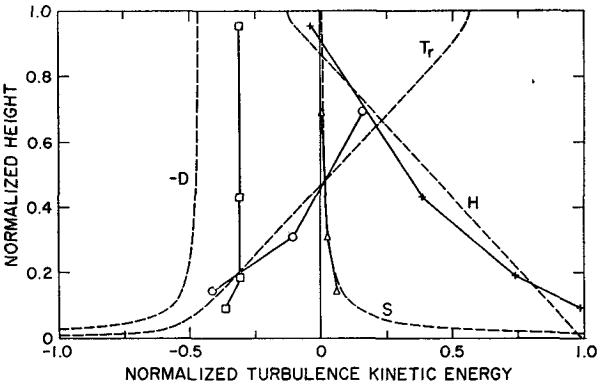

FIG. 5. Normalized terms in the turbulence kinetic energy equation for 25 April 1968. The dashed lines are theoretical curves for the dissipation term (D), the transport term (T_r), the shear-generation term (S), and the buoyancy-generation term (H). The measured values are defined as follows: dissipation rate (□), turbulence energy transport term (○), shear-generation term (△), and buoyancy-generation term (+). The relevant external parameters are given in Table 1.

The vertical transport of kinetic energy was obtained by calculating $\overline{w'e'}$ at each level and dividing the difference between two successive levels by the difference in height. Since this term involves the calculation of a vertical derivative of a third-order moment, the scatter of this term is also larger than for the buoyant production. The vertical transport of pressure fluctuations was not measured.

The rate of dissipation was estimated from the spectral density of the longitudinal velocity, using the

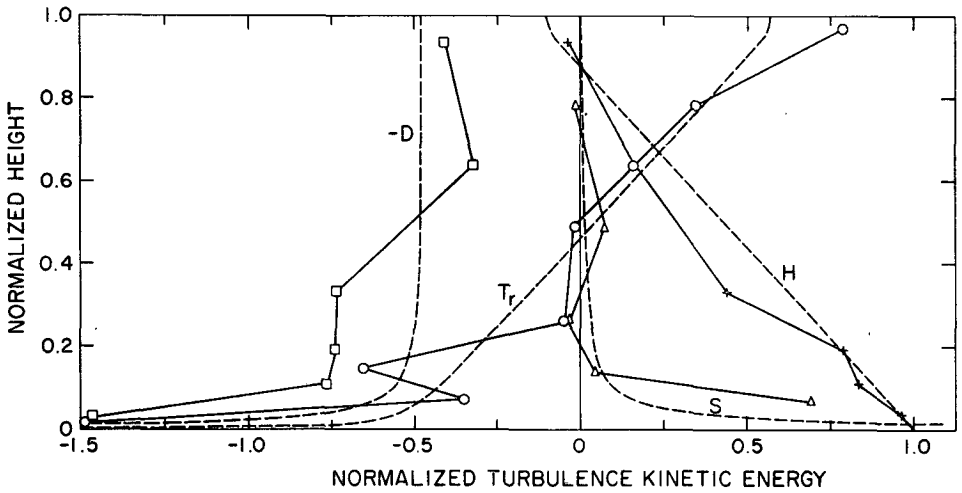

FIG. 6. As in Fig. 5 except for 13 November 1970.

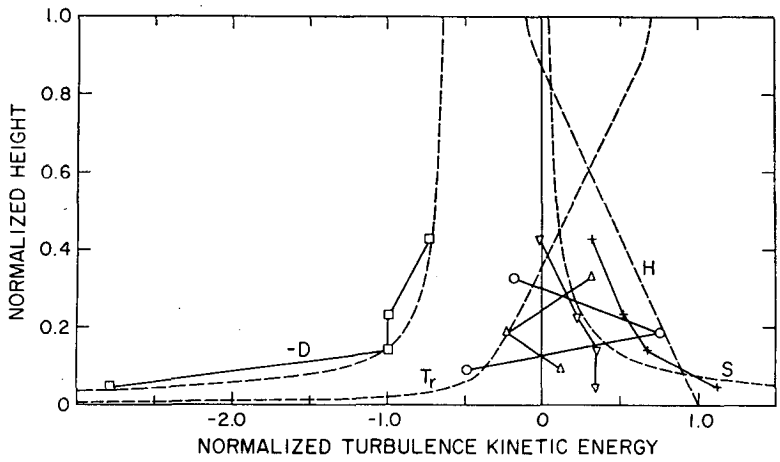

FIG. 7. As in Fig. 5 except for 5 November 1970. In addition, measured values of the horizontal advection of turbulence energy (∇) are shown.

Kolmogoroff hypothesis for the inertial subrange,

$$E(k_1)=a\epsilon^{2/3}k_1^{-5/3}, \tag{19}$$

where $k_1=2\pi/L_x$ and L_x is the wavelength along x. The value $a=0.5$, suggested by Kaimal *et al.* (1972), was used in this equation.

Horizontal advection of turbulence energy was calculated from $\bar{u}$ multiplied by a least-squares determination of the linear trend of the turbulence energy along the direction of the wind.

4. Results of measurements

The measured terms in the turbulence energy budget are presented in Figs. 5, 6 and 7, along with curves obtained from the model presented in Section 2. The relevant boundary layer parameters for the model calculations are given in Table 1. Values of the roughness length z_0 were chosen to be 2 cm over the short-grassland region of eastern Colorado and 0.02 cm over the water. The mean velocity, $\bar{u}_{\text{meas}}$, was obtained from the average of the lowest two levels. Values of $\bar{u}_{\text{calc}}$ were obtained from the integrated formulation for shear, similar to the derivation of (11a), i.e.,

$$\bar{u}_{\text{calc}}=\frac{u_*}{k}(\ln z/z_0-\psi_1), \tag{20}$$

averaged over the lowest two levels. Except for 5 November, $\bar{u}_{\text{meas}}$ and $\bar{u}_{\text{calc}}$ agree very well.

TABLE 1. Values of the relevant boundary layer parameters for the three turbulence kinetic energy budgets presents in Figs. 5, 6, and 7.

	25 April 1968	5 November 1970	13 November 1970
$z_i/-L$	31.5	7.8	38.1
$z_i/z_0\times10^{-5}$	0.52	36	46
z_i (m)	1045	730	912
u_* (cm sec^{-1})	46	37	27
$\bar{u}_{\text{meas}}$ (m sec^{-1})	9.3	10.8	8.4
$\bar{u}_{\text{calc}}$ (m sec^{-1})	9.1	12.3	8.5
$\frac{g}{T}(\overline{w'T_v'})_0$ (cm^2 sec^{-3})	85	16	23.5

The values of the measured dissipation rate in Fig. 5 follow the shape of the theoretical curve but underestimate the theoretical value by about 35%. This is equivalent to an underestimation of the longitudinal velocity spectral density of about 22%, which is larger than the expected error. In Fig. 6, the measured values of dissipation rate are scattered about the theoretical curve. Direct measurements of the rate of dissipation with, for example, an airborne hot-wire anemometer would be very useful for a study of this type.

Measured values of S, H and T_r in both Fig. 5 and 6 agree reasonably well with the theoretical curves. Measured values of T_r do not include the pressure term, although the theoretical curves do.

On 5 November (Fig. 7) the measured values depart significantly from the theoretical curves. This is not surprising in view of the lack of horizontal homogeneity in the boundary layer. The flight pattern started and ended close to the upwind shore and the crosswind legs were 20–30 km from the upwind shore. Two discrete changes occur in the lower boundary at the shoreline: 1) a decrease in surface roughness from a low hilly region with scattered woodlots and buildings to water; and 2) an increase in buoyant production of turbulence energy over the water because of the higher surface temperature of the water, about 4–6C warmer than the land.

The time scale for vertical mixing through the entire boundary layer is proportional to the ratio of the boundary layer height to the convective velocity, $w_*=[(g/T)z_i(\overline{w'T'})_0]^{\frac{1}{3}}$. Deardorff (1970) estimated from a numerical simulation of the boundary layer that

a typical particle circulation time for loops of vertical diameter $>\frac{1}{2}z_i$ was about $3.7z_i/w_*$. On 5 November, this time corresponds to a distance of about 26 km. Much of the time the aircraft was closer than this to shore, so that the boundary layer very likely had not yet adjusted completely to the changed lower boundary. The horizontal advection of turbulence energy, plotted in Fig. 7, indicates that the turbulence energy decreased along the direction of the wind from shore out to about 20 km. At 102 and 167 m (the two middle levels), the advective term is about half as large as H. This may account for the departure of the measured values of T_r and S from the theoretical curves.

Furthermore, $\bar{u}_{\text{calc}}$ on 5 November (Table 1) is larger than $\bar{u}_{\text{meas}}$, thus indicating that the momentum flux is larger than expected over a water surface. Calculating z_0 from (20), upon setting $\bar{u}_{\text{calc}}=\bar{u}_{\text{meas}}$, we obtain $z_0 \approx 0.1$ cm.

Instead of $\overline{w'e'}$ increasing with height to a maximum value about halfway up in the boundary layer as predicted by the theoretical curve and as observed in the other two cases, on 5 November the value at $z_*=0.23$ is less than at $z_*=0.14$. Values of $\overline{w'e'}/w_*^3$ are plotted for all three cases in Fig. 8. The relation between $\overline{w'e'}/w_*^3$ and T_r is

$$\overline{w'e'} \equiv \int_0^z \frac{\partial \overline{w'e'}}{\partial z} dz,$$

$$= -w_*^3 \int_0^{z_*} T_r dz_*. \qquad (21)$$

The solid line in Fig. 8 is the theoretical curve for $\overline{w'e'}$ for free convection, assuming no wind shear throughout the boundary layer while the dashed curve is $\overline{w'e'}/w_*^3$ for 13 November. The measured values for 25 April and 13 November are reasonably close to the theoretical curve, while the values for 5 November are too small at the upper levels. This may again be due to the upper part of the boundary layer not becoming adjusted to the change in the lower boundary. The upper two points are between $\frac{1}{2}$ and $\frac{1}{3}$ as large as predicted by the theoretical curve or, conversely, they are characterized by a buoyancy-generation term $\frac{1}{2}$ to $\frac{1}{3}$ as large as that observed over the water. From these results it appears that the time required for horizontal homogeneity even at relatively low levels in the boundary layer is several times z_i/w_*.

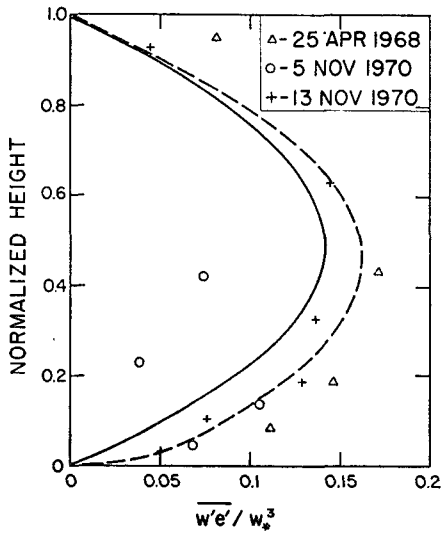

FIG. 8. Normalized vertical flux of turbulence kinetic energy as a function of normalized height. The solid line is the theoretical curve for free convection, the dashed line the theoretical curve for 13 November 1970.

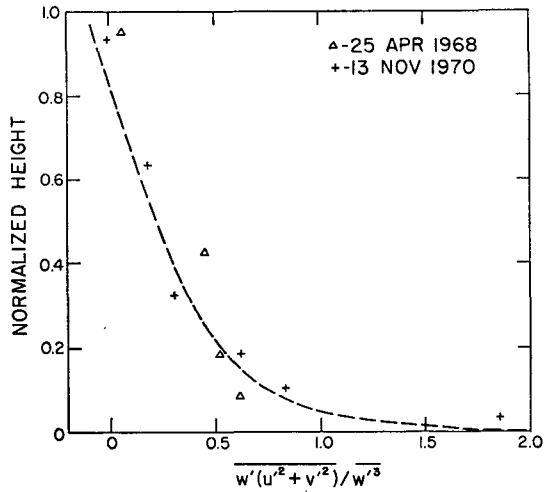

FIG. 9. Ratio of the vertical transport of horizontal turbulence kinetic energy to the vertical transport of vertical turbulence kinetic energy as a function of normalized height. The dashed line is the theoretical curve for 13 November 1970.

The ratio of the horizontal contribution to the vertical flux of turbulence energy, $\overline{w'(u'^2+v'^2)}$, to the vertical contribution, $\overline{w'^3}$, for 25 April and 13 November is plotted in Fig. 9. (The values for 5 November were not plotted because of the large scatter; two of the values were greater than 2.) Wyngaard and Coté (1971) found that in the surface layer, this ratio is about 2; i.e., the contributions of each velocity component are about equal. The aircraft measurements indicate, however, that above the surface layer the relative contribution of $\overline{w'^3}$ increases.

Some preliminary water tank measurements of Willis [the data are as yet unpublished; the experimental setup is described by Deardorff and Willis (1974)] indicate that this ratio in the water tank can be approximated above the lower 10% of its depth by

$$\overline{w'(u'^2+v'^2)}/\overline{w'^3} = -0.55z_*+0.4 = f(z_*). \qquad (22)$$

Since the fluid in the tank, which is heated at the

bottom, has no mean velocity, we assume that (22) represents the free convection limit for this ratio. Similarly, we assume that the result of Wyngaard and Coté (1971) represents the limiting case of shear production of turbulence. On this basis, we assume that $\overline{w'e'}$ can be divided into two terms, one representing the contribution from convection $[(\overline{w'e'})_h]$ and the other from shear $[(\overline{w'e'})_s]$. Therefore, in (15) for T_r, the term $T_{rh}=0.43-H$ represents the contribution from convection and $T_{rs}=0.57(\langle S\rangle-S)/(\langle S\rangle+3.75)$ represents the contribution from shear. We assume that (22) applies to the terms in

$$(\overline{w'e'})_h=\int_0^{z_*} T_{rh}dz_*$$

and that the ratio of horizontal to vertical flux of turbulence energy is equal to 2 for the terms in

$$(\overline{w'e'})_s=\int_0^{z_*} T_{rs}dz_*.$$

The resulting ratio is

$$\frac{f(z_*)\int_0^{z_*} T_{rh}dz_*+\frac{2}{3}[1+f(z_*)]\int_0^{z_*} T_{rh}dz_*}{\int_0^{z_*} T_{rs}dz_*+\frac{1}{3}[1+f(z_*)]\int_0^{z_*} T_{rs}dz_*}. \quad (23)$$

The dashed curve in Fig. 9 is an evaluation of this ratio for 13 November. The measured values agree very well with this curve. We note that as $z_*\to 1$, the ratio approaches 0/0 and thus is not well defined. Qualitatively, however, the ratio approaches zero in the upper part of the boundary layer.

5. Concluding remarks

The measurements presented and discussed in the preceding section show reasonable agreement with the proposed model of the height variation of the terms in the turbulence kinetic energy budget when the unstably stratified boundary layer can be assumed to be horizontally homogeneous. The time required for horizontal homogeneity to be achieved after an abrupt change in the surface roughness and temperature seems to be several times z_i/w_*.

The results indicate that the dissipation rate approaches a constant value in the upper part of the boundary layer ($z\gg -L$), while the transport term increases almost linearly with height to balance the linear decrease of buoyancy generation. The surface layer formulation for shear generation seems to be adequate for including this term in the energy budget throughout almost all the boundary layer since it decreases to less than 10% of the buoyancy term for $z> -4L$, provided $z_i\gg -L$. At the top of the boundary layer, however, this term may again become important.

The greatest uncertainty in the terms of the energy budget is in the region near the top of the boundary layer. Other parameters, such as the wind shear and the lapse rate above the base of the inversion, may be important there. More detailed measurements in this region, as well as more complete sets of measurements through the entire boundary layer for a greater range of $z_i/-L$, would be very useful in testing and possibly extending this model. Direct measurements of the dissipation rate and, if possible, the pressure-transport term would also be desirable.

Acknowledgments. The data used for this study were analyzed by Y. Pann. The aircraft data tape was processed by B. Gacnik. J. Deardorff offered many helpful comments and criticisms throughout the course of this work. I also express my appreciation to the personnel of the NCAR Research Aviation Facility for their efforts during the observational periods.

REFERENCES

Businger, J. A., J. C. Wyngaard, Y. Izumi and E. F. Bradley, 1971: Flux-profile relationships in the atmospheric surface layer. *J. Atmos. Sci.*, **28**, 181–189.

Deardorff, J. W., 1970: Preliminary results from numerical integrations of the unstable planetary boundary layer. *J. Atmos. Sci.*, **27**, 1209–1211.

——, 1972: Numerical investigation of neutral and unstable planetary boundary layers. *J. Atmos. Sci.*, **29**, 91–115.

——, and G. Willis, 1974: The computer and laboratory modeling of the vertical diffusion of nonbuoyant particles in the mixed layer. *Advance in Geophysics*, Vol. 2, New York, Academic Press (in press).

——, —— and D. K. Lilly, 1968: Laboratory investigation on non-steady penetrative convection. *J. Fluid Mech.*, **35**, 7–31.

Kaimal, J. C., J. C. Wyngaard, Y. Izumi and O. R. Coté, 1972: Spectral characteristics of surface layer turbulence. *Quart. J. R. Meteor. Soc.*, **98**, 563–589.

Laufer, J., 1950: Investigation of turbulent flow in a two-dimensional channel. NACA TR-1053, 20 pp.

Lenschow, D. H., 1970: Airplane measurements of planetary boundary layer structure. *J. Appl. Meteor.*, **9**, 874–884.

——, 1971: Vanes for sensing incidence angles of the air from an aircraft. *J. Appl. Meteor.*, **10**, 1339–1343.

——, 1972: The measurement of air velocity and temperature using the NCAR Buffalo aircraft measuring system. NCAR Tech. Note EDD-74, 39 pp.

——, 1973: Two examples of planetary boundary layer modification over the Great Lakes. *J. Atmos. Sci.*, **30**, 568–581.

Myrup, L. O., 1969: Turbulence spectra in stable and convective layers in the free atmosphere. *Tellus*, **21**, 341–354.

Paulson, C. A., 1970: The mathematical representation of wind speed and temperature profiles in the unstable atmospheric surface layer. *J. Appl. Meteor.*, **9**, 857–861.

Rayment, R., 1973: An observational study of the vertical profile of the high frequency fluctuations of the wind in the atmospheric boundary layer. *Boundary-Layer Meteor.*, **3**, 284–300.

Sheih, C. M., H. Tennekes and J. L. Lumley, 1971: Airborne hot-wire measurements of the small-scale structure of atmospheric turbulence. *Phys. Fluids*, **14**, 201–215.

Wyngaard, J., and O. Coté, 1971: The budgets of turbulent kinetic energy and temperature variance in the atmospheric surface layer. *J. Atmos. Sci.*, **28**, 190–201.

Zubkovskiy, S. L., and B. M. Koprov, 1970: On the turbulent energy balance in the boundary layer of the atmosphere. *Izv. Atmos. Oceanic Phys.*, **6**, 989–995.